

EXAFS, XRD and RMC studies of an Amorphous Ga₅₀Se₅₀ Alloy Produced by Mechanical Alloying

K. D. Machado,^{1,*} P. Jóvári,^{2,†} J. C. de Lima,¹ C. E. M. Campos,¹ and T. A. Grandi¹

¹*Departamento de Física, Universidade Federal de Santa Catarina, 88040-900 Florianópolis, SC, Brazil*

²*Hamburger Synchrotronstrahlungslabor HASYLAB am Deutschen*

Elektronen-Synchrotron DESY, Notkestrasse, 85, D-22603, Hamburg, Germany

(Dated: October 12, 2018)

The local atomic order of an amorphous Ga₅₀Se₅₀ alloy produced by Mechanical Alloying (MA) was studied by the Extended X-ray Absorption Fine Structure (EXAFS) and X-ray Diffraction (XRD) techniques and by Reverse Monte Carlo (RMC) simulations of its total x-ray structure factor. The coordination numbers and interatomic distances for the first neighbors were determined by means of EXAFS analysis and RMC simulations. The RMC simulations also furnished the partial pair distribution functions $G_{\text{Ga-Ga}}^{\text{RMC}}(r)$, $G_{\text{Ga-Se}}^{\text{RMC}}(r)$ and $G_{\text{Se-Se}}^{\text{RMC}}(r)$. The results obtained indicated that there are important differences among the local structure of the amorphous Ga₅₀Se₅₀ alloy produced by MA and those of the corresponding crystals, since there are Se-Se pairs in the first coordination shell of the amorphous alloy that are forbidden in the Ga₅₀Se₅₀ crystals.

PACS numbers: 61.10.Ht, 61.10.Eq, 61.43.Bn, 61.43.Dq, 05.10.Ln, 81.05.Gc

In the recent years there has been an increase in the number of applications related to nonlinear optical materials. However, the desired properties concerning this kind of applications, such as optical homogeneity, laser damage threshold, stability of the compound upon exposure to laser beam, ease of fabrication, improved mechanical strength and the possibility of making large crystals are difficult to find in a single material. Some of the materials that can be used for nonlinear applications, like silver gallium selenides, zinc germanium phosphides and thallium arsenic selenides, do not fulfill all of these requirements, limiting severely their efficiency and applicability. Thus, there is a high necessity of developing new materials with a higher level of performance and more cost effective characteristics. Gallium selenide (GaSe) has a number of interesting properties for electrical and nonlinear optics applications. It transmits in the wavelength range varying from 0.65 to 18 μm and its optical absorption coefficient remains below 1 cm^{-1} throughout the transparency range. It has the possibility of converting sum and difference frequencies [1, 2]. It has also been reported to be used in making a number of devices like MOSFET, IR detector, Solar Cell, compound semiconductor, etc. in crystalline form while in amorphous form, it is a potential candidate for optical memory type applications [1, 3]. Crystalline GaSe is a semiconductor of the III-VI family like GaS and InSe and it has a layered graphite type structure with a fourfold layer in the sequence Se-Ga-Ga-Se. The crystal cleaves very easily along the layers [2]. At room temperature, the layers are bound by weak van der Waals-type interactions. The weakness of this interaction explains the existence of a number of polytypes [4]. Ga₅₀Se₅₀ alloys can be prepared by the melting, vapor deposition and molecular beam epitaxy techniques [5, 6, 7, 8]. These techniques have had very limited success because they

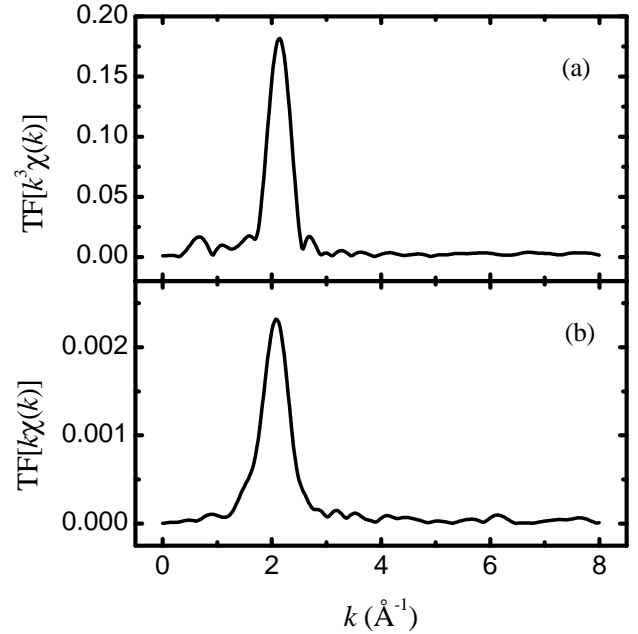


FIG. 1: Fourier transformation of experimental EXAFS spectra: a) at the Ga K-edge and b) at the Se K-edge.

do not have control over the kinetics and morphology. In addition, due to the low melting points of the elemental Ga (30°C) and Se (217°C) and the high vapor pressure of Se above 600°C it is difficult to obtain Ga-Se alloys at specific compositions. On the other hand, the mechanical alloying (MA) technique [9] can be used to overcome these difficulties since the temperatures reached in MA are very low, what reduces reaction kinetics, allowing the production of poorly crystallized or amorphous materials [10, 11, 12, 13] even if the constituents of the alloy have low melting points, as it is in the case of gallium and selenium.

Amorphous $\text{Ga}_{50}\text{Se}_{50}$ ($a\text{-Ga}_{50}\text{Se}_{50}$) was prepared by MA starting from high purity elemental powder selenium (Alfa Aesar, 99.9999% purity, 150 μm) and scraped ingots of gallium (Aldrich, 99.999% purity) with nominal composition $\text{Ga}_{50}\text{Se}_{50}$. The mixture was sealed together with several steel balls into a cylindrical steel vial under argon atmosphere. The ball-to-powder weight ratio was 10:1. A Spex Mixer/Mill model 8000 was used to perform MA at room temperature. The mixture was milled for 15 h. A ventilation system was used to keep the vial temperature close to room temperature. The composition of the alloy was confirmed by an energy dispersive spectroscopy (EDS) measurement and impurity traces were not observed. The alloy produced was investigated by extended x-ray absorption fine structure (EXAFS) and x-ray diffraction (XRD) techniques and also by reverse Monte Carlo simulation (RMC). The EXAFS measurements were carried out on the D04B beam line of LNL (Campinas, Brazil), using a channel cut monochromator (Si 111), two ionization chambers as detectors and a 1 mm entrance slit. All data were taken at room temperature in the transmission mode. The EXAFS oscillations $\chi(k)$ at both K edges, after the standard data reduction procedures using Winxas97 software [14], were Fourier transformed (FT) using a Hanning weighting function within the ranges 3.8 – 14.3 \AA^{-1} for the Ga, and 3.4 – 14.3 \AA^{-1} for the Se edge. They can be seen in Fig. 1. Raw spectra were filtered by Fourier transforming $k^3\chi(k)$ (Ga edge) and $k\chi(k)$ (Se edge) into r -space (Fig. 1) and transforming back the first coordination shells (1.20 – 2.85 \AA for the Ga edge and 1.13 – 3.0 \AA for the Se edge). Filtered spectra were then fit by using Gaussian distributions to represent the homopolar and heteropolar bonds [15]. The amplitude and phase shifts relative to the homopolar and heteropolar bonds needed to fit them were obtained from *ab initio* calculations using the spherical waves method [16] and by the FEFF software. Figure 2 shows the experimental and the fitting results for the Fourier-filtered first shells on the Ga and Se edges. Structural parameters extracted from the fits are listed in Table I. It is interesting to note that the very good fits shown in Fig. 2 were achieved only when Se-Se pairs were considered in the first shell. This fact indicates that the local structure of $a\text{-Ga}_{50}\text{Se}_{50}$ produced by MA is different from its crystalline counterparts as none of the known stable crystalline $\text{Ga}_{50}\text{Se}_{50}$ structures contains Se-Se bonds.

The XRD measurements were carried out at the BW5 beamline [17] at HASYLAB. All data were taken at room temperature. The energy of the incident beam was 121.3 keV ($\lambda = 0.102 \text{\AA}$). The structure factor $S(K)$ (Fig. 3, full line) was computed from the normalized intensity $I(K)$ according to Faber and Ziman [18] and it was modeled by reverse Monte Carlo simulations. This technique is described in details elsewhere [10, 19, 20, 21] and it has been used as a method for structural modeling based directly on experimental data. There are several papers

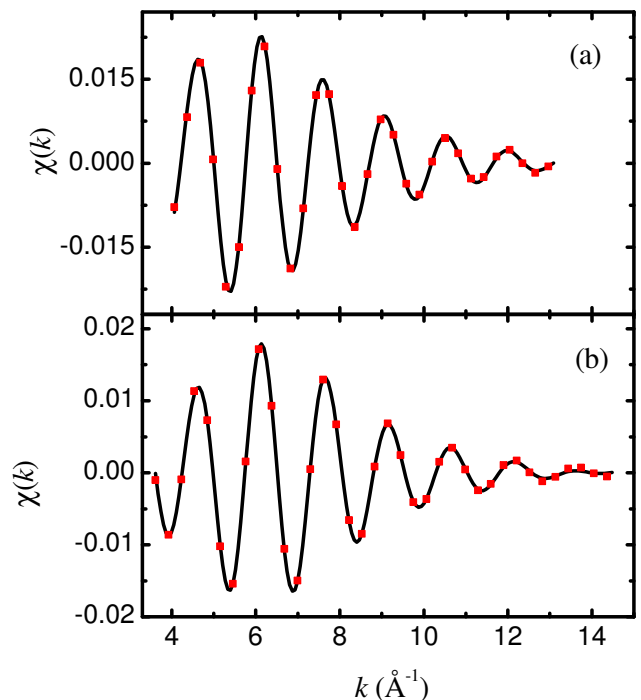


FIG. 2: Fourier-filtered first shell (full line) and its simulation (squares) for $a\text{-Ga}_{50}\text{Se}_{50}$ at the (a) Ga K edge, (b) Se K edge.

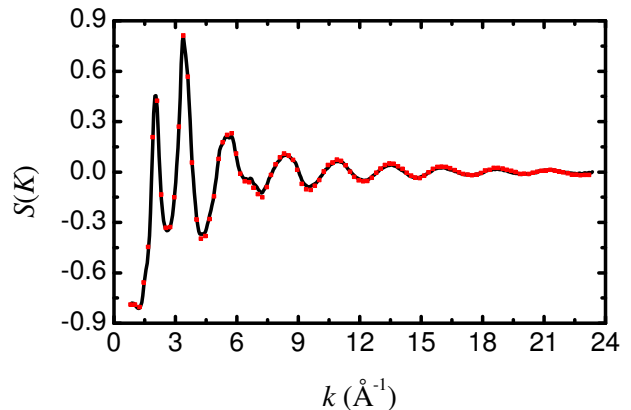


FIG. 3: Experimental (full line) and simulated (squares) total structure factor for $a\text{-Ga}_{50}\text{Se}_{50}$.

[10, 22, 23, 24, 25, 26] reporting structural studies of amorphous alloys by RMC. Simulations were carried out by the RMC program available on the Internet [20]. Cubic cells contained 1600 and 12800 atoms, and the average density was $\rho_0 = 0.03907 \pm 0.0005 \text{ atoms/\AA}^3$. This value was found from the slope of the straight line ($-4\pi\rho_0 r$) fitting the initial part (until the first minimum) of the total $G(r)$ function [27]. The minimum distance of atoms was also extracted from $G(r)$ and fixed at 2.18 \AA . All the simulations were performed considering atoms randomly placed in the cubic cells as starting configurations. Then the following series of simulations were carried out:

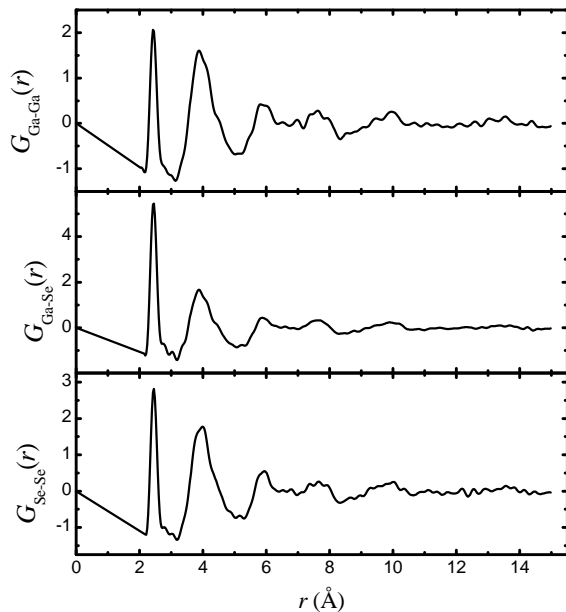


FIG. 4: $G_{\text{Ga-Ga}}^{\text{RMC}}(r)$, $G_{\text{Ga-Se}}^{\text{RMC}}(r)$ and $G_{\text{Se-Se}}^{\text{RMC}}(r)$ functions obtained from the RMC simulations.

1. Hard sphere simulation without experimental data to avoid possible memory effects of the initial configurations in the results.
2. ‘Unconstrained’ runs (i.e. when experimental data were ‘switched on’). These runs led to three essentially identical partial pair correlation functions and partial structure factors which can be considered as linear combinations of the ‘true’ partial quantities. It is to be mentioned that as neither the size nor other *a priori* information can distinguish between Ga and Se atoms at this step no adequate coordination numbers can be obtained.
3. ‘Constrained’ runs. The experimental $\mathcal{S}(K)$ was fit by using EXAFS coordination number values as constraints. Comparison of experimental (full line) and calculated (squares) structure factors for the latter case is shown in Fig. 3 and the partial pair correlation functions (pcf’s) are given in Fig. 4.

Finally the whole series of calculations was repeated from the very beginning with the difference that during the ‘constrained’ run random steps resulting in non-zero Se-Se first coordination number were rejected. It is important to note that if Se-Se pairs are forbidden as first neighbors simulations did not converge, reinforcing the results obtained by EXAFS analysis. The position of the first and second peak are 2.42 Å and 3.89 Å in all of the pcf’s corresponding to a mean bond angle of 107° for the four bond types (Ga-Ga-Ga, Se-Se-Se, Ga-Se-Se, Ga-Ga-Se) that can be directly derived from the pcf peak positions. As this is very close to the value

TABLE I: Structural parameters obtained for α -Ga₅₀Se₅₀.

EXAFS				
	Ga K-edge		Se K-edge	
Bond Type	Ga-Ga	Ga-Se	Se-Ga	Se-Se
N	1.3	2.4	2.4	1.3
r (Å)	2.38	2.45	2.45	2.37
σ^2 (Å ² × 10 ⁻²)	1.58	0.545	0.545	1.77
RMC				
Bond Type	Ga-Ga	Ga-Se	Se-Ga	Se-Se
N	1.2	2.5	2.5	1.3
r (Å)	2.42	2.42	2.42	2.42
Ga ₅₀ Se ₅₀ compound ^a				
Bond Type	Ga-Ga	Ga-Se	Se-Ga	Se-Se
N	1	3	3	6
r (Å)	2.44	2.45	2.45	3.75
Ga ₅₀ Se ₅₀ compound ^b				
Bond Type	Ga-Ga	Ga-Se	Se-Ga	Se-Se
N	1	3	3	6 ^c
r (Å)	2.39	2.47	2.47	3.74

^aSpace group P63/MMC.

^bSpace group P-6M2

^cThe trigonal crystal of space group R3M has 4 Se-Se pairs.

describing perfect tetrahedral coordination (109.5°) and $N_{\text{Ga-Ga}} + N_{\text{Ga-Se}}$ and $N_{\text{Se-Se}} + N_{\text{Se-Ga}}$ are both close to 4 it is evident to assume that ball milled α -Ga₅₀Se₅₀ has a tetrahedral structure with a definite tendency to form homopolar bonds.

The difference of Ga-Ga and Ga-Se bond lengths in the crystalline modifications is not greater than about 0.08 Å (see Table I) and they are also quite close to the value of 2.35 Å found recently for α -Se [22]. As the spatial resolution of diffraction experiments is equal to π/K_{max} the $\mathcal{S}(K)$ factor should be measured at least up to 40 Å⁻¹ or further to get more detailed information on the first coordination shell. It should also be mentioned that due to the value of neutron scattering lengths ($b_{\text{Se}} = 7.970$ fm, $b_{\text{Ga}} = 7.288$ fm) neutron diffraction data would give essentially the same information. Other techniques used to obtain information at the level of pcf’s are either prohibitively expensive (neutron diffraction with isotopic substitution) or yield limited spatial resolution due to the low K_{max} value available (anomalous X-ray scattering).

In summary the local structure of ball milled α -Ga₅₀Se₅₀ was investigated experimentally with EXAFS

and high energy X-ray diffraction. EXAFS analysis led to the following conclusions: the average first coordination number in α -Ga₅₀Se₅₀ is close to 4, Ga and Se local environments are similar and Se-Se bonding is significant. All of these findings were checked and confirmed by RMC study of diffraction data: it was possible to obtain a good fit with coordination constraints close to the EXAFS values while runs without Se-Se first neighbors led to a bad agreement between model and experiment. Mean bond angle calculated from diffraction data is 107° indicating that α -Ga₅₀Se₅₀ has a tetrahedral local structure.

The present study illustrates how complementary information obtained by different experimental techniques can be combined within the frame of reverse Monte Carlo simulation. We believe that this is a useful and efficient way of modelling disordered materials especially in cases when traditional methods (e.g. neutron diffraction with isotopic substitution) are not available.

The Brazilian authors wish to thank the Brazilian agencies CNPq and CAPES for financial support. This study was also partially supported by LNLS (Proposal No. XAS 998/01). P. Jóvári is indebted to Hermann Franz and Martin von Zimmermann (both HASYLAB) for their help during the diffraction measurement.

* Electronic address: kleber@fisica.ufsc.br

† Electronic address: pjovari@mail.desy.de

- [1] N. B. Singh, D. R. Suhre, V. Balakrishna, M. Marable, R. Meyer, N. C. Fernelius, F. Hopkins, and D. Zelmon, *Prog. Cryst. Growth and Char* **37**, 47 (1998).
- [2] N. C. Fernelius, *Prog. Cryst. Growth and Char.* **28**, 275 (1994).
- [3] N. B. Singh, D. R. Suhre, W. Rosch, R. Meyer, M. Marable, N. C. Fernelius, F. K. Hopkins, D. E. Zelmon, and R. Narayanan, *J. Crystal Growth* **198/199**, 588 (1999).
- [4] S. Jandl, J. L. Brebner, and B. M. Powell, *Phys. Rev. B* **13**, 686 (1976).
- [5] A. Ludviksson, L. E. Rumaner, J. W. J. Rogers, and F. S. Ohuchi, *J. Cryst. Growth* **151**, 114 (1995).
- [6] K. Fujita, T. Izumi, K. Ohsaki, T. Tambo, H. Ueba, and C. Tatsuyama, *Thin Solid Films* **247**, 134 (1994).
- [7] S. L. Stoll, E. G. Gillan, and A. R. Barron, *Adv. Materials* **8**, 182 (1996).
- [8] T. L. Ng, N. Maung, G. Fan, I. B. Poole, J. O. Williams, A. C. Wright, D. F. Foster, and D. J. Cole-Hamilton, *Chem. Vapor Deposition* **2**, 185 (1996).
- [9] C. Suryanarayana, *Prog. Mater. Sci.* **46**, 1 (2001).
- [10] K. D. Machado, J. C. de Lima, C. E. M. de Campos, T. A. Grandi, and D. M. Trichês, *Phys. Rev. B* **66**, 094205 (2002).
- [11] C. E. M. Campos, J. C. de Lima, T. A. Grandi, K. D. Machado, and P. S. Pizani, *Sol. State. Commun.* **123**, 179 (2002).
- [12] C. E. M. Campos, J. C. de Lima, T. A. Grandi, K. D. Machado, and P. S. Pizani, *Physica B* **324**, 409 (2002).
- [13] J. C. de Lima, V. H. F. dos Santos, and T. A. Grandi, *Nanostruct. Matter.* **11**, 51 (1999).
- [14] T. Ressler, *J. Phys.* **7**, C2 (1997), licensed to LNLS.
- [15] E. A. Stern, D. E. Sayers, and F. W. Lytle, *Phys. Rev. B* **11**, 4836 (1975).
- [16] J. J. Rehr, *J. Am. Chem. Soc.* **113**, 5135 (1991).
- [17] H. F. Poulsen, J. Neufeind, H.-B. Neumann, J. R. Schneider, and M. D. Zeidler, *J. Non-Cryst. Solids* **188**, 63 (1995).
- [18] T. E. Faber and J. M. Ziman, *Philos. Mag.* **11** (1965).
- [19] R. L. McGreevy and L. Pusztai, *Mol. Simulations* **1**, 359 (1988).
- [20] RMCA version 3, R. L. McGreevy, M. A. Howe and J. D. Wicks, 1993. available at <http://www.studsvik.uu.se>.
- [21] R. L. McGreevy, *J. Phys.: Condens. Matter* **13**, 877 (2001).
- [22] P. Jóvári and L. Pusztai, *Phys. Rev. B* **64**, 14205 (2001).
- [23] D. A. Keen and R. L. McGreevy, *Nature* **344**, 423 (1990).
- [24] Y. Wang, K. Lu, and C. Li, *Phys. Rev. Lett.* **79** (1997).
- [25] M. Bionducci, G. Navarra, R. Bellissent, G. Concas, and F. Congiu, *J. Non-Cryst. Solids* **250**, 605 (1999).
- [26] A. D. Cicco, M. Taglienti, M. Minicucci, and A. Filipponi, *Phys. Rev. B* **62**, 12001 (2000).
- [27] Y. Waseda, *The Structure of Non-Crystalline Materials (Liquid and Amorphous Solids)* (McGraw-Hill, New York, 1980).